Journal of Engineering Science and Technology
Vol. 11, No. 1 (2016) 109 - 120

EFFECT OF DIFFERENT HEAT EXCHANGERS ON THE WASTE-HEAT DRIVEN THERMOACOUSTIC ENGINE

DAVID W. Y. KHOO, YOUSIF A. ABAKR*

Department of Mechanical, Manufacturing and Materials Engineering, The University of Nottingham Malaysia Campus, Jalan Broga, 43500 Semenyih, Selangor Darul Ehsan, Malaysia
*Corresponding Author: yousif.abakr@nottingham.edu.my

Abstract

To enhance the efficiency of the SCORE thermoacoustic engine, it is important to investigate the heat transfer between the bulge or the convolution and the regenerator. Heat transfer due to convection has great influence on performance of the thermoacoustic engine. The total heat transfer from the bulge or the convolution to the first few layers of the regenerator is mainly due to convection and radiation. In this paper, the two modes of heat transfers, convection and radiation are under investigation numerically. The main objective of the present study is to find an ideal shape of the bulge which transports heat from the cooking stove to regenerator. Four different designs of the bulge are proposed in this work. Numerical method Fluent^{TM} CFD modelling with surface to surface (S2S) radiation method is chosen to study the radiation effect. The main challenge in the development of the models of such system is to simulate the coupled heat transfer effect and the temperature gradient across both the bulge and porous media surfaces. The results show a very limited amount of heat transfer by convection on all the bulge simulated cases, with a dominant radiative heat transfer over the convective heat transfer while convection was found to be dominant in the convolution simulated case. By looking at the heat fluxes solely, convolution design is recommended to improve the engine performance as it possesses higher total heat flux comparatively but most of it was found to be by convection rather than radiation. The results were validated analytically in a recent accepted paper and found to be in good agreement. To accurately predict the heat transfer in the model, conduction must also be included in future studies as well.

Keywords: Thermoacoustic, Heat transfer, Regenerator, Convolution, Radiation heat flux.

Nomenclatures

A	Area, m^2
C_p	Specific heat capacity, J/(kgK)
E	Emissive power of the surface, W/m^2
f	Frequency, Hz
F	View factor
J	Radiosity, W/m^2
k	Thermal conductivity, W/(Km)
P	Pressure, Pa
q_{in}	Energy flux incident on the surface, W/m^2
q_{out}	Energy flux leaving the surface, W/m^2
t	Time, s
T	Temperature, K
v	Velocity, m/s
w	Angular velocity, rad/s

Greek Symbols

μ	Dynamic viscosity, kg/(ms)
ε	Emissivity
ρ	Density, kg/m^3

Abbreviations

TAE	Thermo-Acoustic Engine
SCORE	Stove for Cooking, Refrigeration and Electricity
CFD	Computational Fluid Dynamics
UDF	User Defined Function
RANS	Reynolds Averaged Navier Stokes
SIMPLE	Semi Implicit Method for Pressure Linked Equations
S2S	Surface-to-Surface

1. Introduction

Thermoacoustic heat engine is a device which uses a temperature difference to induce high-amplitude sound waves [1, 2]. In general, it is a device that converts heat energy to sound energy or vice-versa. The fundamental components of a typical thermoacoustic heat engine include a resonance tube, a regenerator and heat exchangers. SCORE successfully demonstrated the potential development of low cost thermoacoustic engines for rural communities in the past few years [3, 4]. The recent focus of SCORE engine is to make use of wood instead of propane as heat source to generate electricity. The essential components of the thermoacoustic driver of the SCORE engine are illustrated schematically in Fig. 1.

In order to enhance the efficiency of the engine, which is crucial for maximising the overall engine performance, it is important to investigate the heat transfer between the regenerator and the bulge (or convolution). Despite experimental studies of SCORE show only radiative heat transfer, heat transfer due to convection has great influence on the total heat transfer of the engine as well. Ignoring such mode of heat transfer may yield inaccuracies in estimating the overall heat transfer. In this paper, two modes of heat transfers, convection and radiation are investigated numerically.

The main objective of the present study is to find an ideal shape of the bulge which transports heat from the flames to regenerator. A three-dimensional model is proposed and implemented in a computational fluid dynamics (CFD) simulation environment. The simulations are obtained by solving the governing equations using the commercially available Fluent^{TM} Software 6.3 [5]. The model is further examined by developing three additional geometries which have different bulge designs. The geometry of the first model of the bulge is essentially a semi-circular cylinder. The rest of the models of the bulge were designed based on the first bulge design but segmented into a smaller semi circles. In the recent SCORE Demo 2 engine design, the bulge is substituted by a convolution which believed to have a better heat transfer to the regenerator of the engine [6, 7].

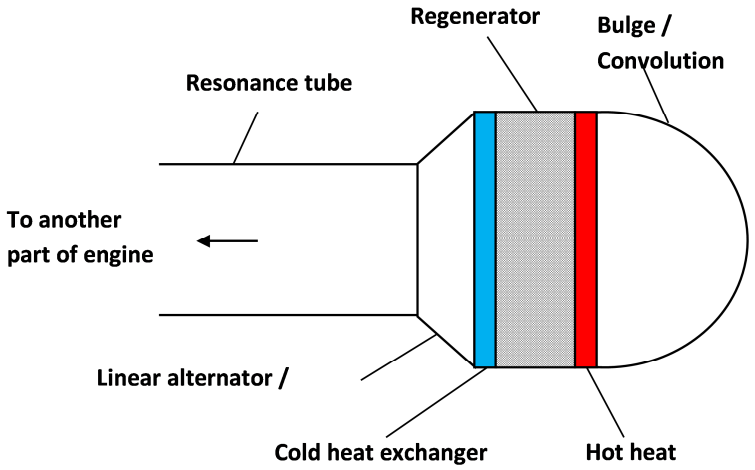

Fig. 1. Basic components of the SCORE engine driver integrity.

Most of the heat is assumed to be transferred from the convolution to the regenerator by convection and radiation. Thus, the main challenge in the development of such system models is to simulate the coupled heat transfer effect and the temperature gradient from the bulge to the porous media (regenerator) top surface. The most significant advantage of using Fluent^{TM} to model such application is that the innumerable fluid models already implemented by it can be efficiently utilised to predict the coupled heat transfer performance. Moreover, the User Defined Function (UDF) allows for applying any required boundary conditions easily, where the thermally induced acoustic flow of the engine can be defined as an inlet oscillating pressure boundary condition.

Forced convection is induced in the system using an oscillating pressure inlet boundary condition. An ideal gas approximation is used as an assumption. The temperature therein is high, ranging from 674 K at the top surface of the regenerator to 1024 K at the surface of the bulge or the convolution. The numerical results for temperature profiles and heat transfer were found for the different models and the comparison of the results were used to determine which model will have better performance. Surface to surface (S2S) radiation model is used to model the heat transfer in this study. The simulation model can be treated

as an enclosed space which has complicated heat transfer by the fact that fluid in the enclosure, in general, is oscillating. And due to the convection effects the fluid adjacent to the hotter surface rises and the fluid adjacent to the cooler one falls, setting a rotational motion within the enclosure that enhances convection heat transfer through the enclosure. The thermally induced acoustic waves are initialised using user defined function as a periodic flow of the inlet pressure boundary condition. In the following sections of this paper, more detailed 3D governing equations and numerical algorithm will be described.

2. Numerical Approach

There are total four different cases, each represents a different geometry in terms of variation of mesh and size. The geometries of the simulation models were first created in the Gambit software. The simulated space consists of mainly two regions; one is the porous zone (regenerator) and the other is the bulge (or convolution) region. The first few layers of the regenerator near the bulge are basically acted as the hot heat exchanger. A two-dimensional (XY plane), schematic convolution simulation model together with its dimension (in mm) is shown in Fig. 2. The physical dimensions of the model presented are taken directly from the SCORE experimental data.

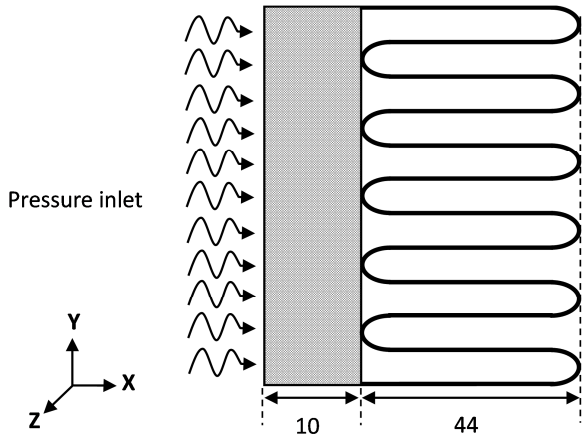

Fig. 2. The XY plane of the schematic convolution.

All the bulge dimensions are constructed in such a way that all the simulation models possess the same bulge surface areas 0.0628 m^2 except the one-semicircular cylinder bulge model which has the same total bulge volume with the convolution model. The porous region dimensions for all the geometries are the same; each of 200 mm length, 200 mm width and 10 mm thickness. The two surfaces on the z-direction were assumed to be adiabatic wall on one side and an opening on the opposite one. The mesh generated for the geometries are to precisely determine the heat flow of the simulation models. In order to accurately simulate the models, hexahedral mesh is used to mesh the volume of all the four geometries. Meanwhile at the wall, it is made up of quadrilateral meshes which are expected to give better results over a mesh with full triangular grids. Uniform

mesh or constant mesh spacing is generated for the geometries. These apply to both the porous and bulge regions. Table 1 shows the actual numbers of nodes and cells for each of the cases.

Table 1. Numbers of nodes and cells, effective bulge surface area and total bulge volume excluding the porous media (generator) for all the four geometries.

Type of geometry	No. Cells	No. Nodes	Effective bulge surface area / m^2	Total bulge volume / m^3
One-semicircular cylinder	101100	107508	0.0424	0.00123
One-semicircular cylinder	45604	49977	0.0628	0.00557
One-semicircular cylinder	181200	193035	0.0628	0.001184
Convolution	565760	620055	0.231	0.00123

In order to supply a periodic flow for the model, a user defined function (UDF) was developed in C programming language. A harmonic pressure wave Eq. (1) presented was used as an inlet pressure with the aid of user defined function (UDF) in Fluent™.

$$P = P_o + Asin(wt) \quad (1)$$

The time average pressure, P_o = 670 Pa was taken as the operating pressure. The coefficient A = 100 Pa is the pressure amplitude; $w = 2\pi f$ is the angular velocity and f = 80 Hz is the operating frequency of the model. The temperature of the periodic inlet pressure is assumed to have a constant temperature of 674 K. On the other hand, at the bulge surface, the temperature is set to be 1024 K based on the SCORE experimental data. Constant emissivity, ε of 0.78 and no-slip boundary condition are assigned to all the stainless steel walls.

The most widely used and validated model, standard k-ε model was selected as the turbulence model to account for both the porous media and heat transfer. Thermal effects were also taken into consideration to enhance the heat transfer calculations near the walls. The Reynolds-Averaged Navier Stokes (RANS) equations are used in this work; Fluent™ solves numerically the usual Continuity, Momentum and Energy equations [8,9]. Fluent solver uses a finite-volume procedure, which converts the governing different equation into algebraic form, together with the SIMPLE (Semi-Implicit-Method for Pressure Linked Equations) algorithm to solve these quantities numerically. For the discretization of the equations the second-order upwind scheme is selected for all the turbulent flow simulations carried out. A list of settings for the CFD model is presented in Table 2.

Surface-to-surface (S2S) model was chosen to model the radiative heat transfer in this study. This model presents a method to obtain the intensity field of radiation exchange in an enclosure of gray-diffuse surfaces. The energy exchange between two surfaces depends on their size, separation distance, and orientation. These parameters are accounted for by the view factors [10]. The main assumption of S2S model is that the exchange of radiative energy between surfaces is unaffected by the medium that separates them. Any absorption, emission or scattering of radiation can be ignored so only "surface-to-surface' radiation needs to be considered for analysis. The S2S model assumes that all

surfaces are gray and diffuse. Thus according to the gray body model, if a certain amount of radiant energy (E) is incident on a surface, then a fraction (ρE) is reflected, a fraction (αE) is absorbed, and a fraction (τE) is transmitted. This radiation model also assumes that the heat transfer surfaces are opaque to thermal radiation. The transmissivity, therefore can be neglected. In follows, from the conservation of energy that the emissivity (ε) = absorptivity (α) and that reflectivity (ρ) = 1 - emissivity (ε). The energy flux leaving a given surface is composed of directly emitted and reflected energy. The reflected energy flux is dependent on the incident energy flux from the surroundings, which then can be expressed in terms of the energy flux leaving all other surfaces. Fluent™ uses the following Eq. (2) for the energy reflected from surface k [10]:

$$q_{out,k} = \epsilon_k \sigma T_k^4 + \rho_k q_{in,k} \quad (2)$$

where $q_{out,k}$ is the energy flux leaving the surface, ε_k is the emissivity, σ is the Boltzman's constant and $q_{in,k}$ is the energy flux incident on the surface from the surroundings.

Table 2. Fluent™ settings for all the four geometries.

Solver			Unsteady
Viscous model			k-ε
Gravity			-ve 9.81 ms^{-2} in the Y direction
Material	**Fluid**		Ideal Gas Approximation
	Solid		Stainless steel ρ = 7800 kgm^{-3} . C_p = 510 $Jkg^{-1}K^{-1}$, k = 21.4 $Wm^{-1}K^{-1}$
Boundary condition	**Pressure inlet**		User Defined Function
	Bulge wall	**0.001 m**	T = 1024 K , ε = 0.78
	Adiabatic wall	**wall thickness**	ε = 0.78 (do not participate in S2S Radiation
Discretisation schemes			Pressure: 2nd Order Upwind Density: 2nd Order Upwind Momentum: 2nd Order Upwind Turbulent Kinetic Energy: 2nd Order Upwind Turbulent Dissipation Rate: 2nd Order Upwind Energy: 2nd Order Upwind Pressure-Velocity Coupling: SIMPLE

The amount of incident energy upon a surface from another surface is a direct function of the S2S view factor, F_{jk} . The view factor, F_{jk} is the fraction of energy leaving surface k that is incident on surface j. The incident energy flux $q_{in,k}$ can be expressed in terms of the energy flux leaving all other surfaces as Eq. (3) [5] :

$$A_k q_{in,k} = \sum_{j=1}^{N} A_j q_{out,j} F_{jk} \quad (3)$$

where A_k is the area of surface k and F_{jk} is the view factor between surface k and j (N is the number of surfaces).

On another form of the aforementioned equation, Fluent™ utilises the radiosity J equation. The total energy given off a surface k is given by Eq. (4) [5]:

$$J_k = E_k + \rho_k \sum_{j=1}^{N} F_{kj} J_j \quad (4)$$

where E_k represents the emissive power of surface k.

3. Modelling of the Regenerator

According to the SCORE experimental data, the regenerator comprises of 56 layers of stainless steel wire mesh which has a total thickness size of 10 mm. The material properties used for the porous zone is the same as the walls. A volumetric porosity, σ is as 0.792 based on the SCORE experimental data. The current study uses superficial velocity inside the porous media, based on volumetric flow rate, to ensure continuity of the velocity vectors across the porous media interface. Laminar zone option is disabled so that turbulence effect in porous media will also be taken under consideration. The effect of the porous media on the turbulence field is only approximated. In essence, the porous media is nothing more than an added momentum sink in the governing momentum equations. The porous media is modelled using addition of a momentum source term to the standard fluid flow equations. Equation (5) shows the source term composes of two parts; a viscous loss term and an inertia loss term [11]:

$$S_i = -\left(\sum_{j=1}^{3} D_{ij} \mu v_j + \sum_{j=1}^{3} C_{ij} \frac{1}{2} \rho |v| v_j\right) \quad (5)$$

where S_i is the source term for i th (x, y or z) momentum equation, v_j is the velocity component in j th (x, y or z) direction, $|v|$ is the velocity magnitude and μ is the fluid viscosity. The inertial and viscous resistance factors used in this work are derived based on the SCORE experimental results [12] as tabulated in Table 3.

Table 3. The SCORE experimental results.

Data No.	Zone	Average gas particle displacement / mm	Velocity / ms^{-1}	Pressure / Pa	Pressure drop / Pa
1	Porous	2	1.01	447.2	2.36
	Bulge	8	4.02	444.8	-
2	Porous	3	1.52	670.8	4
	Bulge	12	6.03	667.2	-
3	Porous	4	2.02	894.4	4.72
	Bulge	16	8.04	889.6	-
4	Porous	7.1	3.57	1578.3	243.8
	Bulge	24	12.06	1334.5	-
5	Porous	14.2	7.12	3156.6	487.7
	Bulge	48	24.12	2668.9	-

The Reynolds number at the bulge region ranges from 5×10^4 to 3×10^5. The dependence between the pressure drop, Δp and velocity, v in the porous zone is approximated based on experimental correlation as Eq. (6):

$$\Delta p = 7.43v^2 + 17.4v \quad (6)$$

Leading to pressure drop as Eq. (7):

$$\Delta p = 7.43 \frac{kg}{m^3} v^2 + 17.4 \frac{kg}{m^2 s}\, v \tag{7}$$

In the case of simple homogenous porous media, the momentum source term S_i for the porous media is defined as Eq. (8) [13]:

$$S_i = -\left(\frac{\mu}{\alpha} v_i + C_2 \frac{1}{2} \rho v_i^2\right) \tag{8}$$

where α and C_2 are defined as the permeability and the inertial resistance factor of the porous medium respectively.

For all cases considered in these simulations the convergence criterion or normalised residual for the governing equations is set to be 1*e*-06. Transient simulations have a fixed time step size of 0.03142 seconds so that 20 time steps will complete a full period of oscillation in the inlet pressure. The maximum iterations per time step is set to be 20 which is sufficient to yield accurate results.

4. Results and Discussion

The results of the simulation were obtained based on the previous settings for the four stated conditions. Contours of temperature distribution at XY plane were plotted for all the cases. From the plots it was found that the temperature of the air near the hot surface of the bulge is very high, but the temperature of the air away from the hot surface is relatively low for all the bulge cases, when this is compared to the convolution, it is found that the temperature of the air between the straight surfaces of the convolution is very hot, it is even hotter than the top surface of the regenerator. This behaviour may enhance convection versus radiation, which is not good for the performance of the engine, this is illustrated in Fig. 3, which depicts the preliminary temperature distribution of the geometries along the X direction when t = 7.9 seconds. The temperature profiles are taken from YZ plane using area-weighted average method. As shown in Fig. 3, a general trend can be seen. All the geometries show a gradual increase in temperature towards the bulge except the convolution which has an intense high temperature affecting big air volume away from the porous media.

The convection and radiative heat fluxes from the surface of the bulge in the first three cases and for the convolution were plotted and compared to each other. The cases of all the semi-circular sections (one, two and four semi-circular sections) showed a heat transfer by radiation in the range of 30000 Wm^{-2} to 48000 Wm^{-2}. As depicted in Fig. 4, the convection heat flux prediction of the first three cases is very close with an average value of approximately 4000 Wm^{-2}. From the comparison of both modes of heat transfer it is clear that that most of the heat is transferred by radiation in the first three cases.

Moreover, the study of two modes of heat transfer for the convolution was also carried out as shown in Fig. 5. It can be observed that the heat transfer by radiation is only a small fraction of the total heat flux. This indicates again that the current design of the convolution promotes convection heat transfer over radiation heat transfer. The convolution case showed a very high convection heat flux especially beside the straight walls, this proves that the convolution will have strong convection heat transfer to the air trapped within the convolutes. Figure 6 demonstrates the expected region which has greater

radiative heat transfer in the convolution. This makes physical sense because majority heats are radiating to themselves.

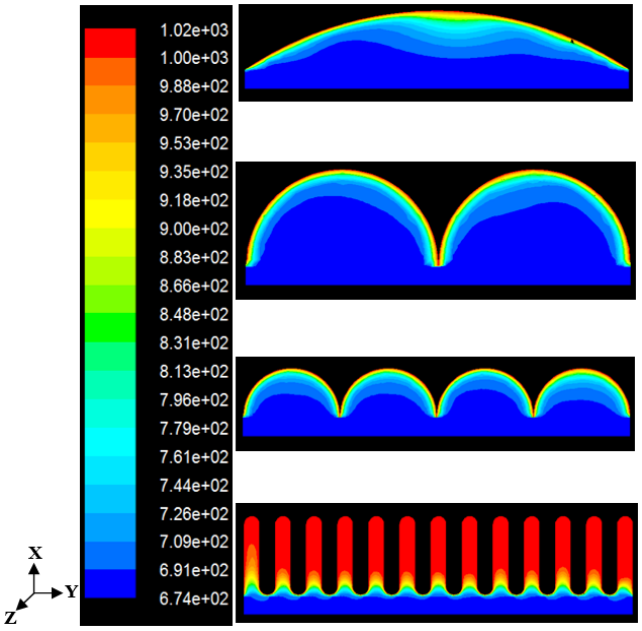

Fig. 3. Contour of temperature distribution at XY plane when Z = 0.1 m for all the geometries at *t* = 7.9 seconds.

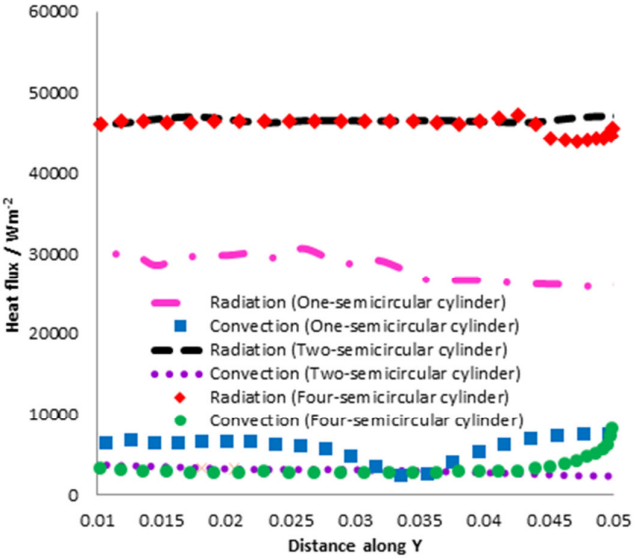

Fig. 4. Convection heat flux and radiation heat flux for one-semicircular cylinder, two-semicircular cylinder and four-semicircular cylinder at Z = 0.1 m on the bulge surface at *t* = 15.7 s when the bulge surface temperature is 1024 K.

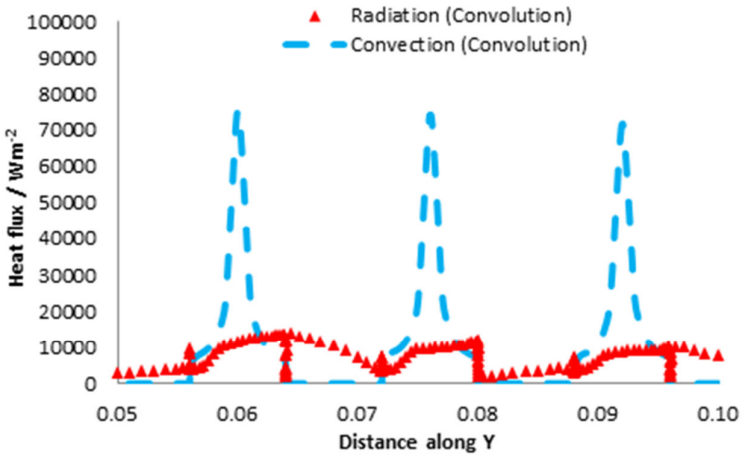

Fig. 5. Convection heat flux and radiation heat flux for convolution at Z = 0.1 m on the convolution surface at *t* = 15.7 s when the convolution surface temperature is 1024 K.

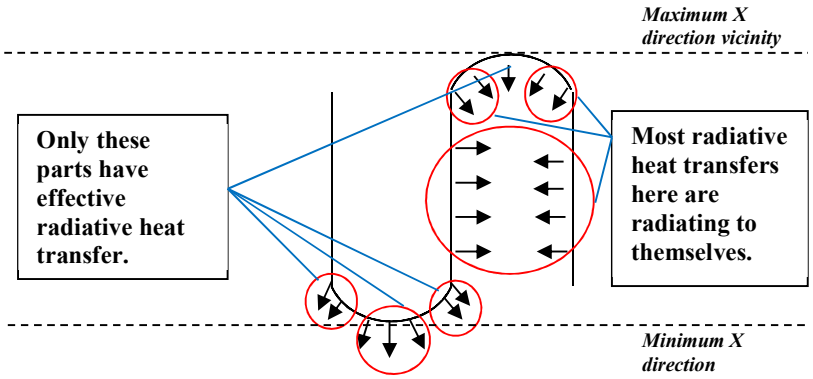

Fig. 6. The cross-section of the convolution model.

5. Conclusions

This work examines the feasibility of a new approach of studying the heat transfer in the SCORE engine using CFD analysis. In this approach, numerical method Fluent^{TM} CFD modelling with S2S radiation method is chosen to study the radiation effect. This paper presents the results of two modes of heat transfer, namely radiation and convection to support the selection of the ideal shape of bulge. Based on the results obtained, the design of the bulge showed more radiation versus convection to the regenerator top surface. The total amount of heat transferred from the convolution was found to be greater than that of all the bulge cases, but most of it was found to be by convection rather than radiation. It is also noticed that there was a relatively huge amount of air volume at high temperature due to its proximity to the larger surface area of the convolution. To accurately predict the heat transfer in the model, conduction must also be included

as well. Neglecting conduction heat transfer will result in underestimating the temperature and heat flux which will lead to the miscalculation of total heat flux and etcetera. The CFD simulation carried out here have shown that some operating parameters and properties can be of crucial importance in the heat transfer process between the hot surface subjected to the flames and the receiving top surface of the regenerator. The results obtained were validated against analytical solutions in the recent accepted paper and indicated good agreement [14]. In future, the numerical models will be refined through the inclusion of an appropriate atmospheric pressure and by validation with the experimental results.

Acknowledgements

The authors would like to extend thanks to MOSTI funds for funding this work.

References

1. Swift, G.W. (2002). *Thermoacoustic: A Unifying Perspective for some Engines and Refrigerators*. Acoustic Society of America.
2. Abakr, Y.A.; Al-Atabi, M.T.; and Chen, B. (2011). The influence of wave patterns and frequency on thermo-acoustic cooling effect. *Journal of Engineering Science and Technology*, 6(3), 392-396.
3. Saha, C.R.; Riley, P.H.; Paul, P.; Yu, Z.; Jaworski, A.J.; and Johnson, C.M. (2012). Halbach array linear alternator for thermo-acoustic engine. *Sensors and Actuators*, 178, 179-187.
4. Riley, P.H.; Saha, C.R.; and Johnson C.M. (2010). Designing a Low-Cost, Electricity Generating Cooking Stove. *Technology and Society Magazine IEEE*, Summer.
5. Fluent Inc. (2006). *Fluent 6.3 User's Guide*.
6. Khoo, D.W.Y.; Abakr, Y.A.; and Ghazali, N.M. (2012). Numerical investigation on the heat transfer from the cooking stove to the thermoacoustic engine's regenerator. *International conference, low-cost, electricity generating heat engines for rural areas*. Nottingham, UK.
7. Khoo, D.W.Y.; Abakr, Y.A.; and Ghazali, N.M. (2013). Cfd investigation of the heat transfer between an external heat source and the regenerator of a thermoacoustic engine. *Elsevier Procedia Engineering*, 56, 842-848.
8. Neale, A.; Derome, D.; Blocken, B.; and Carmeliet, J. (2007). Coupled Simulation of Vapor Flow between Air and a Porous Material. *Buildings X Proceedings*. Florida, USA.
9. Bharath, M.S.; Singh, B.; and Aswathanarayana, P.A. (2010). Performance Studies of Catalytic Converter Used in Automobile Exhaust System. *The 37th International Conference on Fluid Mechanics and Fluid Power*. Chennai, India.
10. Qashou, I.; Tafreshi, H.V.; Pourdeyhimi, B. (2009). An Investigation of the Radiative Heat Transfer through Nonwoven Fibrous Materials. *Journal of Engineered Fibers and Fabrics*, 4(1), 9-15.
11. Yan, Y.; Uddin, R.; and Sobh, N. (2005). CFD Simulation of a Research Reactor. *American Nuclear Society Topical Meeting in Mathematics and Computations*. Avignon, France.

12. SCORE (2007). www.score.uk.com
13. Banjare, Y.P.; Sahoo, R.K.; and Sarangi, S.K. (2009). CFD simulation of a Gifford–McMahon type Pulse Tube Refrigerator. *International Journal of Thermal Sciences*, 48(12), 2280-2287.
14. Khoo, D.W.Y.; Abakr, Y.A.; and Ghazali, N.M. (2014). Radiation heat transfer between the externally heated surface and the regenerator of the thermoacoustic engine. *Elsevier Energy Procedia*, 61, 2576-2579.